HHS Public Access

Author manuscript

Acta Biomater. Author manuscript; available in PMC 2017 January 15.

Published in final edited form as:

Acta Biomater. 2016 January 15; 30: 212–221. doi:10.1016/j.actbio.2015.11.024.

A Micro-architecturally Biomimetic Collagen Template for Mesenchymal Condensation Based Cartilage Regeneration

Mousa Younesi[1], **Victor M. Goldberg**[2,✡], and **Ozan Akkus**[1,3,*]

[1]Department of Mechanical and Aerospace Engineering, Case Western Reserve University, Cleveland, OH 44106, USA

[2]Department of Orthopedics Case Western Reserve University Cleveland, OH 44106, USA

[3]Department of Biomedical Engineering, Case Western Reserve University, Cleveland, OH 44106, USA

Abstract

The unique arcade-like orientation of collagen fibers enables cartilage to bear mechanical loads. In this study continuous-length aligned collagen threads were woven to emulate the interdigitated arcade structure of the cartilage. The weaving pattern provided a macropore network within which micromass cell pellets were seeded to take advantage of mesenchymal condensation driven chondrogenesis. Compression tests showed that the baseline scaffold had a modulus of 0.83 ± 0.39 MPa at a porosity of 80%. The modulus of pellet seeded scaffolds increased by 60% to 1.33 ± 0.37 MPa after 28 days of culture, converging to the modulus of the native cartilage. The scaffolds displayed duress under displacement controlled low-cycle fatigue at 15% strain amplitude such that load reduction stabilized at 8% after 4500 cycles of loading. The woven structure demonstrated a substantial elastic recoil where 40% mechanical strain was close to completely recovered following unloading. A robust chondrogenesis was observed as evidenced by positive staining for GAGs and type II collagen and aggrecan. Dimethyl methylene blue and sircol assays showed GAGs and collagen productions to increase from 3.36 ± 1.24 and 31.46 ± 3.22 at day 3 to 56.61 ± 12.12 and 136.70 ± 12.29 μg/μg of DNA at day 28 of culture. This woven collagen scaffold holds a significant potential for cartilage regeneration with shorter *in vitro* culture periods due to functionally sufficient mechanical robustness at the baseline. In conclusion, the mimicry of cartilage's arcade architecture resulted in substantial improvement of mechanical function while enabling one of the first pellet delivery platforms enabled by a macroporous network.

Graphical abstract

*Corresponding author: oxa@case.edu.

✡Prof. Victor M. Goldberg passed away on February 7, 2015 before he was able to review this manuscript. He has contributed intellectually to the design of experiments and the interpretation of data. He was a co-author in several conference abstracts which were related to this manuscript. We dedicate this paper to his memory and long standing service and leadership in orthopaedic research. He will be missed greatly.

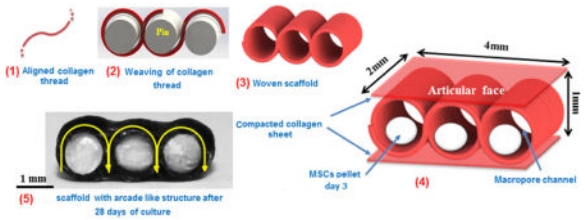

Keywords

electrochemical compaction; woven scaffold; collagen; mesenchymal cell condensation; chondrogenesis; cartilage tissue engineering

1. Introduction

Cartilage is a load-bearing tissue which facilitates low-friction articulation in diarthroidal joints. Decades of duty cycles and limited self-regeneration capacity take their toll on cartilage integrity, resulting in the formation of defects [1]. Cartilage defects are repaired by microfracturing, mosaicplasty or chondrocyte transplantation. Microfracturing results in mechanically inferior fibrocartilage formation [2]. Mosaicplasty may result in donor site morbidity and healing seams [3]. Chondrocyte transplantation is limited to the repair of small defects and clinical trials report mixed outcomes [4, 5]. Therefore, regenerative medicine approaches are needed to restore functionality of damaged cartilage.

Chondrocytes and stem cells from various sources (marrow, adipose, embryonic, *etc.*) have been used in cartilage TE. While chondrocytes perform better than mesenchymal stem cells in terms of generating a cartilage-like matrix [6, 7], finding sufficient donor tissue and maintaining the chondrocytic phenotype during *in vitro* expansion remain as challenges [8–10]. The challenge with mesenchymal stem cells (MSCs) has been the attainment of stable chondrogenic differentiation [11]. What appears to induce chondrogenesis of MSCs relatively reliably is high density cell seeding [12, 13] during which MSCs undergo condensation and cell-cell adhesions are conducive to chondrogenesis. Formation of neocartilage during embryogenesis also occurs through a similar mesenchymal condensation process [14, 15]. While such scaffold free strategies have met with some success; weak mechanical properties, extended culture time [16] and demanding bioreactor strategies to provide strength and shape to the high density condensate increase the cost and time [17].

Since condensation is critical to the attainment of chondrogenesis, a scaffold system which enables the delivery of MSCs in pellet form would unify the chondrogenic merit of condensation with the structural merits of scaffolds. Cell pellets, at sufficient numbers for appropriate condensation [16], are sized at hundreds of microns to a millimeter. Therefore, a scaffold that can deliver high density condensates need to be macroporous. Attaining sufficient mechanics while accommodating high levels of ordered porosity requires a special material, with a sophisticated microstructure. To the best of our knowledge, there has been no reports of scaffold systems designed to deliver cell pellets.

Electrochemical processing of collagen solutions addresses the poor mechanics of collagen products by compacting and aligning collagen solutions as threads whose strength is among the strongest of collagen biomaterials (50–100 MPa) [18–21]. Previous work used such high strength collagen threads to fabricate woven scaffolds for tendon and ligament tissue engineering [22, 23]. Weaving patterns of this scaffold and other woven scaffolds [24] do not entail macroscale porosity; thus, they do not allow for pellet seeding.

In this study, a macroporous scaffold was woven from electrocompacted collagen threads to accommodate cell-pellets. The weaving pattern mimicked some of the architectural characteristics of the native arcade-like orientation patterns of collagen fibers in cartilage. In our strategy, the woven scaffold was purely a mechanical crucible for protecting and delivering cell pellets in mechanically robust environment. Chondrogenesis was attained by mesenchymal condensation and TGFβ-3. Combination of mesenchymal condensation driven chondrogenesis within a load-bearing scaffold as such may help expedite repair timeline in the future by enabling earlier implantation of the scaffold framework.

2. Materials and methods

2.1. Scaffold Fabrication

Scaffold production is comprised of 3 steps. In the first step collagen thread is produced by electrochemical alignment process as explained in previous publications [22, 25]. Briefly, acid solubilized collagen molecules (3 mg/mL) are dialyzed against deionized water. Following dialysis, the solution is applied between two stainless steel electrode wires (1.8 mm separation) in an electrochemical cell (Fig.1a). Electrical currents generate a pH gradient in the electrochemical cell. Collagen molecules acquire positive charge near the cathode and negative charge near the anode. Electrorepulsion by electrodes compact the collagen molecules at the isoelectric point of the electrochemical cell where the net charges of the collagen molecules are zero. Our prior work also demonstrated that the longer axes of collagen molecules are oriented parallel to the longer axis of the thread [26]. We used this principle in the design of a device to fabricate the aligned collagen threads in continuous length [22]. The diameters of the threads were 0.11 ± .03 mm.

Uncrosslinked collagen threads were then woven in a zig-zag pattern around a set of equidistant pins with 1 mm diameter (Fig.1b). The weaving pattern of the scaffold (Fig 1c) mimicked the arcade structure of cartilage (Fig.2 a & b) such that the molecular orientation of collagen was parallel to the plane of the surface and became vertically oriented by mid thickness of the scaffold.

In the second step, two planar graphite electrodes were used to fabricate electrochemically compacted collagen sheets (Fig.1c). One compacted collagen sheet was placed each on the top and the bottom of the woven pattern. These sheets served to stabilize the threads together.

In the third step, the threads and the sheets were crosslinked in genipin solution (0.625% w/v in 90/10 v/v ethanol and water mixed solution) for 72 hrs [19]. Following crosslinking, the pins were removed, leaving behind cylindrical pores of 1 mm diameter to be populated by

cell pellets (Fig. 1d). Scaffolds were washed thoroughly with deionized water, dehydrated and stored at 4 °C until use. The nominal dimensions of resulting scaffolds were 4 × 2 × 1 mm in width, depth and height (Fig 1c).

2.2. Polarized microscopy

Collagen fiber orientation in collagen threads and woven scaffold were visualized via polarized light optical microscope (Olympus BX51). An articular cartilage sample from lamb knee joint was utilized to compare the collagen fiber orientation thorough the thickness of cartilage and the woven scaffold.

2.3. Mechanical tests

2.3.1. Compressive Mechanical Properties—Woven scaffolds were prepared with dimensions of 4 mm × 2 mm × 1 mm and were soaked in 1x phosphate buffered saline (PBS) one hour before testing. Samples were subjected to constant strain-rate (1%/s) compression (Rheometrics Solid Analyzer RSAII, Rheometrics Inc., Piscataway, NJ, USA). The samples were highly resilient and did not fail; therefore, stress values reached by 10% strain are reported as maximum compressive stress. Apparent Young's modulus was determined by calculating the slope of stress-strain curve in the range of 3% to 6% strain by linear regression. The mean values were calculated from five samples (n = 5). Bovine and rabbit cartilage samples were cut from the distal femoral condyles using a 5 mm biopsy punch. Cartilage samples were also soaked in PBS about 1 hr before compression tests and tested as described for collagen samples.

2.3.2. Fatigue test—Scaffolds were tested in cyclic mode using a servo-controlled fatigue test machine (Test Resources 800L, Minnetonka, MN). Tests were performed under strain control up to 4500 cycles under a sinusoidal loading mode with frequency of 1 Hz and at a maximum strain value of 15%. This value is selected because it is in the natural strain range experienced by cartilage and is used in bioreactors for mechanical stimulation [27, 28]. Under strain control, the load decreased with increasing number of cycles, with greater amplitude of reduction implying a greater degree of degradation of fatigue performance. Five samples were tested and mean and standard deviation of the loads are reported at different cycles. Samples were kept hydrated during testing by drop-wise application of PBS.

2.4. *In Vitro* Mesenchymal Condensation

For cell culture, samples were disinfected with 70% ethanol overnight, washed three times (each 20 mins) with deionized water and treated with high glucose Dulbecco's Modified Eagle Medium (DMEM) at 37 °C for 1 hr. Bone marrow derived human mesenchymal stem cells at passage zero were obtained from Case Western Reserve University Cancer Center under IRB approval. The cells were cultured on T-75 culture flasks (Corning, Corning, NY) at a density of 5000 cells/cm^2 and cultured at 37 °C at 5% CO_2. The expansion medium was consisted of low glucose DMEM (life technology), 10% fetal bovine serum (Gibco, life technology), 1% penicillin–streptomycin–Fungizone (Gibco), and 10 ng/mL basic recombinant human fibroblast growth factor (hFGF) (R&D Systems, Minneapolis, MN). Medium was replaced every 3 days until cells became 85% confluent. At this time they were

trypsinized (0.25% trypsin–ethylenediaminetetraacetic acid; Gibco), resuspended in DMEM +10% FBS+ 1% penicillin–streptomycin–Fungizone, counted with a hemacytometer, and seeded again. Passage three cells were pelletized. Cells were suspended in media at a concentration of 1,000,000 cells/mL and spun at 500g for 12 mins. Cell pellets were cultured for 3 days without disturbing them so that they gained sufficient consistency to be transferred to the scaffold using tweezers. At this time point the pellet size is 0.6 ± 0.2 mm as measured by Caliper. One pellet was placed in each channel of the scaffold (Fig.2). Scaffolds were cultured in low-attachment 24-well plates (Corning) in 1.0 mL of culture medium per well consisting of DMEM–high glucose (Gibco, life technology), 1% minimum essential amino acid (Gibco, life technology), 1% sodium pyruvate (Gibco, life technology), 50 μg/mL ascorbic-2-phosphate (Sigma-Aldrich, St. Louis, MO), 1% insulin, transferrin, selenous acid (ITS) premix (Corning, Discovery labware, Inc.), 40 ng/mL dexamethasone and 1% penicillin–streptomycin (Gibco, life technology) which was supplemented with 10 ng/mL TGF-β3. The media were changed every 2 days. Scaffolds were analyzed at 3, 14, and 28-day time points to assess chondrogenic development in scaffold. Free standing pellets were cultured as positive controls to determine whether chondrogenesis is affected within the confines of the scaffold.

2.5. Histology and immunohistochemistry

On days 3, 14, and 28 samples were fixed with 10% formalin solution at room temperature for histology and immunohistochemistry. Fixed samples were taken through a series of increasing ethanol solutions and xylene steps to clear the constructs. Samples were then embedded in paraffin and cut into 5 μm sections. General histological staining of hematoxylin and eosin (H&E), safranin O, and masson-trichrome were performed on xylene-cleared sections to highlight cell morphology, GAGs and collagen production, respectively. Immunostaining for type I, type II, and Type X collagen and Aggrecan were performed using monoclonal antibodies to these collagen types (abcam, MA, US.). and aggrecan (abcam, MA, US) Briefly, unstained 5 μm-sections were prepared from paraffin blocks and baked for 30 minutes at 60° C in a Boekel Lab oven. The slides were then processed using a BondMax Automated Immunostainer (Leica). The slides were deparaffinized, antigen retrieved with Bond Enzyme Pretreatment Kit (Leica) for 10 minutes at room temperature. Sections were incubated in primary antibodies for 15 mins and subsequently counterstained onboard with the automated instrument. The Bond Polymer Refine Red Detection System (Leica Biosystems) was used for detection.

2.6. Glycosaminoglycan (GAG) content quantification

Samples on day 3, 14, and 28 were bleached in 3 M guanidine hydrochloride/0.05M Tris-HCl buffer (pH = 7.5) and mixed with a shaker at 4°C overnight. Extracted solutions were dialyzed against 1x (Tris-buffered saline) TBS overnight and stored at −20 °C for measurement. 0.1 mL of samples was mixed with 0.1 mL of the DMMB staining solution (40 μM) in a 96 well-plate. Every sample was prepared in triplicate. Chondroitin sulfate from bovine trachea (Sigma-Aldrich) was used as standard. Serial dilution of the standard solution was prepared by mixing 0.1 mL of standard solution at the concentration of 10 μg/mL with 0.1 mL of buffer solution. The plate was scanned by a micro-plate reader (Spectramax M2, Molecular Devices) at the wavelength of 525 nm. Absorbance values were

recorded and plotted versus the concentrations for standard samples and based on the standard values the amount of GAGs in experimental samples were calculated and reported as amount of GAG per cell number in pellet at day 3.

2.7. Collagen content quantification

Samples were treated in pepsin/acid solution at a concentration of 0.1 mg/mL of 0.5 M acetic acid at 4 °C overnight to solubilize cell made collagen. Using the Sircol assay protocol for collagen quantification (Sircol Soluble Collagen Assay, Biocolor Life Science Assays) the standard samples and experimental samples for measurement were prepared and placed in a 96 well-plate. A micro-plate reader (Spectramax M2, Molecular Devices) was used to measure the absorbance of the samples at 555 nm wavelength. Collagen amount in samples were calculated by using the calibration curve plotted based on standard samples absorbance and reported as amount of collagen per cell number in pellet at day 3. All samples were repeated in triplet and mean values were reported.

2.8. Statistical analysis

Data obtained in this study were reported as mean ± standard deviation. Mechanical test data were analyzed with one-way ANOVA with Tukey's pairwise comparison to determine significant differences between blank scaffolds, cell seeded scaffolds and native cartilages. Differences in DNA content, GAGs content and collagen production of were performed using general linear method (GLM) General linear model statistical analysis was performed to analyze association of weight increase, GAG and collagen product of free-standing pellets vs. scaffold seeded pellets over time. Based on the general linear model analysis results, weight increase, GAG and collagen product over time were statistically analyzed using one-way ANOVA test with Tukey's pairwise comparison (Minitab 16 software, Minitab Inc., State College, PA). Statistical significance is set at 95% confidence level for all tests ($p < 0.05$). Error bars in figures represent the standard deviations of the means.

3. Results

Results of polarized optical microscopy demonstrated the horizontal (parallel to articular surface) orientation of the collagen fibers in superficial region of cartilage and the woven scaffold. Collagen fibers' orientation changed gradually to a vertical orientation in the deeper region of the cartilage and scaffold (Figure 2a & b). This change in orientation is visualized via polarized microscopy as the colors of different regions with different fiber orientations will be different. In superficial region the horizontal orientation of the fibers appeared in blue color while the deeper region with vertical orientation appeared in orange color both in cartilage and in the scaffold (Figure 2a & b).

Stress-strain curves of scaffolds seeded with pellets after 28 days of culture showed higher modulus and compressive stress values than empty scaffolds (Fig. 3a). The compressive stress of empty scaffolds at 10% strain was 90.8 ± 17.2 kPa while the scaffolds seeded with pellet presented a compressive stress of 118.7 ± 29.8 kPa. Furthermore, the Young's modulus of the scaffold increased from 0.83 ± 0.39 MPa for empty scaffolds to 1.33 ± 0.37 MPa for pellet seeded scaffolds after 28 days of culture, corresponding to 60% increase (Fig.

3b). The mean compressive modulus of pellet seeded scaffolds was significantly greater ($P<0.05$) than that of the rabbit cartilage and below that of the bovine cartilage.

Under strain controlled fatigue, the scaffold preserved 92% of its baseline load value after 4500 cycles (Fig. 3c). Woven scaffolds demonstrated a substantial elastic recoil capability. When loaded up to 40% strain and unloaded, the scaffolds recovered 90% of total strain (Fig.4a–c).

Cell number in pellet seeded scaffolds did not change notably over time as evidenced by relatively stagnant DNA content both for free standing pellets and for pellets seeded within the scaffolds (Fig. 5a). Similar to free standing pellets, the weights of pellet seeded scaffolds increased significantly ($P<0.05$) over 28 days (Fig. 5b). Pellet seeded scaffold weight increased by 37% up to day 14 of culture and 87% up to day 28 of culture (Fig.5b). H&E staining of the pellet seeded scaffolds at different time points illustrated that the size of cell pellets increase over time via synthesizing a cartilage like matrix and filled the scaffold pores partially to completely over 28 day of culture (Fig. 6a). High magnification images of H&E stained scaffolds at day 28 showed (Fig. 6b) cells to have round morphologies with presence of extracellular matrix in the pericellular space. Blue filaments in Masson-trichrome staining (Fig. 6c) illustrated the production of the collagen by cells. The intensity of blue in Masson-trichrome stained sections increased gradually by day 28. Safranin O staining (Fig. 7a) of samples showed that cells produced GAGs in scaffold by day 14 and increasingly so by day 28 as evidenced by higher staining intensity. Presence of type II collagen in cells pellets was confirmed via immunostaining (Fig. 7c). The intensity and amount of red stain significantly increased from day 1 to day 28 which is a sign of increasing deposition of collagen II in the pellets by cells.

DMMB assay for quantification of GAGs content in scaffolds showed an increase over 28 days of culture (Fig. 8a). The amount of GAGs increased from 3.37 ± 1.25 μg per μg of DNA in scaffold at day 3 to 20.2 ± 2.83 μg per μg of DNA and 56.6 ± 12.13 μg per μg of DNA at days 14 and 28 in scaffold, respectively. These amounts were close to those of cells made in pellet form with no significant differences. Sircol assay showed same results for collagen produced by cells in scaffolds (Fig. 8b). Amount of collagen in pellet seeded scaffolds increased significantly over time: 31.4 ± 3.2, 46.2 ± 8.7, and 136.7 ± 12.3 μg of collagen per μg of DNA at days 3, 14, 28, respectively. Collagen amounts in free standing pellets changed similarly over time and were not significantly different from pellets seeded in scaffolds. Immunostaining of the scaffold at day 28 confirmed the presence of aggrecan (Fig. 9a). Immunostaining of the scaffold at day 28 for type I collagen was weakly positive and for type X collagen was negative (Fig. 9b & C) indicating that cells differentiated to the chondrogenic lineage with no evidence of endochondral ossification as of day 28.

4. Discussion

An essential feature in designing the scaffold is porosity and pore interconnectivity because they allow for initial cell seeding throughout the scaffold. Interconnected porosity also facilitate cell–cell interactions, nutrient transfer and removal of metabolic byproducts, and tissue growth [29]. Lien et al. [30] showed small pores to favor cellular proliferation and big

pore size to promote (ECM) production. The presented woven scaffold had a high percentage of macro pore volume fraction (~80 %) which enabled cell pellet seeding. Importantly, the woven scaffold was able to sustain a mechanical performance on par with the native cartilage despite this high level of porosity. Relative stagnancy in DNA content over time while tripling of scaffold weight indicated that the growth of pellets to occur by ECM synthesis, enabled by the sizeable pore space.

A scaffold must maintain its structural integrity and stability during fabrication, clinical handling, and fixation at the implant site [31]. Moreover, it should protect the embedded cells from mechanical stresses and withstand the in vivo loading environment until the newly formed tissue can assume the load-bearing function. The scaffold material should provide a desirable environment for biological activities such as cell attachment, proliferation, differentiation, and cell–cell interaction [29, 31, 32]. Results of mechanical tests showed that the compressive mechanical properties of designed woven scaffold matches those of native cartilage. The compressive modulus of woven scaffold 0.83 ± 0.39 MPa for empty scaffold and 1.33 ± 0.37 MPa for pellet seeded scaffold. Human cartilage compressive modulus, based on other works [24, 33], is in range of 0.4 to 0.8 MPa which is in close agreement with designed woven cartilage. The mechanical robustness of scaffold without cells would reduce the mechanical demand from the early stage seeded cell pellet, resulting in reduced in vitro conditioning time prior to *in vivo use*. Scaffold strength and modulus improved after 28 days of cell culture, indicating that cell pellets grow and fill the scaffold pore space and contribute to the mechanical strength of the scaffold.

Physiological loads during the physical activities like walking and running, including those experienced in the articular joints, are mostly cyclic in nature. Therefore, cartilage needs to be resilient under fatigue. The majority of cartilage tissue engineering studies report static properties, due in part, to low fatigue resistance of scaffold materials or cell-made tissues in scaffold free strategies. Besides fatigue, a scaffold should have a high capacity to recover elastic strain. High amount of permanent deformation would distort the conformity between the scaffold and the defect and also may result in damage to the resident cells. Liao et al. [34] showed that a composite woven scaffold can recover 78% of the applied strain (7.8% out of 10% strain). The reported recovery took 10 minutes after unloading. Woven collagen scaffold presented in this study was able to recover 90% of the strain which was applied at very high levels (36% out of 40% strain). The recovery occurred within 10 s.

There are various factors which endowed the current scaffold with superior mechanical function. First, aligned collagen threads making up the scaffold has a high level Young’s modulus of about 600 MPa [19]. Second, the weaving scheme emulated several aspects of the Benninghoff arcades observed in native cartilage (Fig. 2). However, a limitation of the arcade structure in this study was that the spacing between arcades was at the order of magnitude of mm whereas arcades in cartilage tissue are closely spaced. Still, the presence of arcades provided resilience under compression. It is important to emphasize that collagen threads were woven in the uncrosslinked form and they were crosslinked with the pins in place. Therefore, the circular arcade conformation was permanently programmed into the fabric. The weaving pattern results in interdigitation of arcades which should facilitate load transfer and load sharing between threads. Another mechanism which facilitates distribution

of load between threads is the placement and crosslinking of the sheet above and below the woven scaffold. All these facets mimic some of the essential microarchitectural characteristics of cartilage arcade and result in favorable resiliency and fatigue performance of the woven collagen scaffold. One aspect of the scaffold that differs from the cartilage is that the cartilage fibers approach the subchondral face perpendicularly whereas the scaffold fibers do not. This limitation can be addressed in the future by changing the weaving pattern by using a set of pins with different cross-sectional shape other than circular pins to provide us with vertically oriented collagen threads at the bottom of the scaffold. Also, a second parallel woven layer can be introduced by using a scaffold that is woven by collagen/hydroxyapatite threads to promote the growth of supporting bone layer beneath the engineered cartilage layer.

In this work immunostaining indicated strongly positive Collagen type II and slightly positive staining for Collagen type I at day 28 of culture. Relative abundance of type II collagen signals robust chondrogenesis. Previous studies showed before overt chondrogenesis, undifferentiated mesenchymal cells produce a transient ECM that functions to temporally regulate both their aggregation and differentiation into chondrocytes. Both in vivo and in vitro, this precartilage matrix is defined by a unique composition of molecules residing in the extracellular space, including collagen types I, II [14, 15, 35]. Although collagen type I is not found in mature hyaline cartilage ECM, it may play vital roles in regulating both mesenchymal condensation and chondrogenic differentiation. Dessau et al. [36] used immunohistochemistry to show that, before the onset of overt chondrogenesis in the embryonic chick limb, mesenchymal progenitor cells secrete an ECM rich in collagen type I. Moreover, as these prechondrocytes cells progress through the act of mesenchymal condensation, their production of collagen type I increases. However, as overt chondrogenesis begins and the newly differentiated chondroblasts commence expression of mature hyaline cartilage matrix molecules, production of collagen type I stops. The weak staining for type I collagen in our scaffolds may be remnant from the prechondrogenic stage.

When considering the application of MSCs in cartilage repair, it is important to evaluate the risk of chondrogenic stability which in some cases may transition in to endochondral ossification. Type X collagen is thought to play a role in the transformation of cartilage into bone [37–40] because of its presence in hypertrophic cartilage and its calcium binding properties. Our results showed collagen type X was not present in cell-made ECM (Fig. 9c) with abundance of cartilage specific molecules of aggrecan (Fig. 9b). Therefore, a robust chondrogenesis is present in this scaffold model with no indication of endochondral ossification as of day 28. Longer term culture periods will be needed to further augment this conclusion.

High magnification of H&E staining image of the woven scaffold (Fig.10a) shows the round cell morphology which is a key feature of chondrocytes. As the pellets growth inside the scaffold's holes, cells located at the perimeter of pellets attach and diffuse inside the gaps between collagen threads. One limitation of the current scaffold is such that the weaving pattern does not allow for the easy fusion of pellets laterally. Future improvements in the weaving pattern can address this problem. Specifically the weaving scheme would have a skip pattern as illustrated in Fig.10b to introduce lateral connection between neighboring

channels through which the pellets can fuse laterally. Such a weaving pattern is likely to reduce the strength and stiffness, requiring a compromise between lateral fusion and mechanical performance.

4. Conclusion

In this study a novel woven scaffold concept made from pure collagen threads was introduced. The macrostructure of the scaffold mimicked the arcade structure of the cartilage and mechanical performance of the scaffold converged to that of natural cartilage despite very high volume fraction of macroporosity. The scaffold provided a framework which enabled cell pellet condensation process to enhance chondrogenesis. The scaffold provided mechanical robustness throughout the 28 days of *in vitro* culture during which pellets have grown in size predominantly by extracellular matrix production that is rich in collagen II and GAGs. Cell made ECM contributed meaningfully and significantly to the mechanics of the scaffold. Results illustrated the chondrogenesis of the pellet seeded cells inside the scaffold with comparable performance with cells pellet outside the scaffold, indicating that the confinement within the proposed scaffold does not alter the natural course of mesenchymal condensation. We expect such scaffolds with high level of baseline mechanical robustness to shorten the time of conditioning the cell seeded scaffold prior to *in vivo* use.

Acknowledgments

We thank Amad Awadallah for assistance in histology and immunohistochemistry and Yunus Alapan for assistance in imaging. The study was partially funded by National Institutes of Health (Grant Number R01 AR063701) and the AO Foundation.

References

1. Hunziker EB. Articular cartilage repair: basic science and clinical progress. A review of the current status and prospects. Osteoarthritis and cartilage/OARS, Osteoarthritis Research Society. 2002; 10:432–63.
2. O'Driscoll SW. The healing and regeneration of articular cartilage. Journal of Bone and Joint Surgery-American Volume. 1998; 80A:1795–812.
3. Hangody L, Kish G, Karpati Z, Szerb I, Udvarhelyi I. Arthroscopic autogenous osteochondral mosaicplasty for the treatment of femoral condylar articular defects. A preliminary report. Knee Surg Sports Traumatol Arthrosc. 1997; 5:262–7. [PubMed: 9430578]
4. Kon E, Verdonk P, Condello V, Delcogliano M, Dhollander A, Filardo G, et al. Matrix-assisted autologous chondrocyte transplantation for the repair of cartilage defects of the knee: systematic clinical data review and study quality analysis. Am J Sports Med. 2009; 37(Suppl 1):156S–66S. [PubMed: 19861700]
5. Magnussen RA, Dunn WR, Carey JL, Spindler KP. Treatment of focal articular cartilage defects in the knee: a systematic review. Clin Orthop Relat Res. 2008; 466:952–62. [PubMed: 18196358]
6. Connelly JT, Wilson CG, Levenston ME. Characterization of proteoglycan production and processing by chondrocytes and BMSCs in tissue engineered constructs. Osteoarthritis and cartilage/OARS, Osteoarthritis Research Society. 2008; 16:1092–100.
7. Erickson IE, Huang AH, Chung C, Li RT, Burdick JA, Mauck RL. Differential maturation and structure-function relationships in mesenchymal stem cell- and chondrocyte-seeded hydrogels. Tissue Eng Part A. 2009; 15:1041–52. [PubMed: 19119920]
8. Knutsen G, Engebretsen L, Ludvigsen TC, Drogset JO, Grontvedt T, Solheim E, et al. Autologous chondrocyte implantation compared with microfracture in the knee - A randomized trial. Journal of Bone and Joint Surgery-American Volume. 2004; 86A:455–64.

9. Stokes DG, Liu G, Coimbra IB, Piera-Velazquez S, Crowl RM, Jimenez SA. Assessment of the gene expression profile of differentiated and dedifferentiated human fetal chondrocytes by microarray analysis. Arthritis and Rheumatism. 2002; 46:404–19. [PubMed: 11840443]
10. Thirion S, Berenbaum F. Culture and phenotyping of chondrocytes in primary culture. Methods Mol Med. 2004; 100:1–14. [PubMed: 15280583]
11. Mauck RL, Yuan X, Tuan RS. Chondrogenic differentiation and functional maturation of bovine mesenchymal stem cells in long-term agarose culture. Osteoarthritis and cartilage/OARS, Osteoarthritis Research Society. 2006; 14:179–89.
12. Mackay AM, Beck SC, Murphy JM, Barry FP, Chichester CO, Pittenger MF. Chondrogenic differentiation of cultured human mesenchymal stem cells from marrow. Tissue Eng. 1998; 4:415–28. [PubMed: 9916173]
13. Murdoch AD, Grady LM, Ablett MP, Katopodi T, Meadows RS, Hardingham TE. Chondrogenic differentiation of human bone marrow stem cells in transwell cultures: generation of scaffold-free cartilage. Stem Cells. 2007; 25:2786–96. [PubMed: 17656642]
14. Hall BK, Miyake T. All for one and one for all: condensations and the initiation of skeletal development. BioEssays: news and reviews in molecular, cellular and developmental biology. 2000; 22:138–47.
15. DeLise AM, Fischer L, Tuan RS. Cellular interactions and signaling in cartilage development. Osteoarthritis and cartilage/OARS, Osteoarthritis Research Society. 2000; 8:309–34.
16. Bhumiratana S, Eton RE, Oungoulian SR, Wan LQ, Ateshian GA, Vunjak-Novakovic G. Large, stratified, and mechanically functional human cartilage grown in vitro by mesenchymal condensation. Proc Natl Acad Sci U S A. 2014; 111:6940–5. [PubMed: 24778247]
17. Raghunath J, Rollo J, Sales KM, Butler PE, Seifalian AM. Biomaterials and scaffold design: key to tissue-engineering cartilage. Biotechnol Appl Biochem. 2007; 46:73–84. [PubMed: 17227284]
18. Cheng XG, Gurkan UA, Dehen CJ, Tate MP, Hillhouse HW, Simpson GJ, et al. An electrochemical fabrication process for the assembly of anisotropically oriented collagen bundles. Biomaterials. 2008; 29:3278–88. [PubMed: 18472155]
19. Uquillas JA, Kishore V, Akkus O. Genipin crosslinking elevates the strength of electrochemically aligned collagen to the level of tendons. Journal of the Mechanical Behavior of Biomedical Materials. 2012; 15:176–89. [PubMed: 23032437]
20. Islam A, Chapin K, Younesi M, Akkus O. Computer aided biomanufacturing of mechanically robust pure collagen meshes with controlled macroporosity. Biofabrication. 2015; 7:035005. [PubMed: 26200002]
21. Younesi M, Islam A, Kishore V, Panit S, Akkus O. Fabrication of compositionally and topographically complex robust tissue forms by 3D-electrochemical compaction of collagen. Biofabrication. 2015; 7:035001. [PubMed: 26069162]
22. Younesi M, I A, Kishore V, Anderson JM, Akkus O. Tenogenic Induction of Human MSCs by Anisotropically Aligned Collagen Biotextiles. Advanced Functional Materials. 2014; 24
23. Islam A, Bohl MS, Tsai AG, Younesi M, Gillespie R, Akkus O. Biomechanical evaluation of a novel suturing scheme for grafting load-bearing collagen scaffolds for rotator cuff repair. Clinical biomechanics. 2015; 30:669–75. [PubMed: 26009492]
24. Moutos FT, Freed LE, Guilak F. A biomimetic three-dimensional woven composite scaffold for functional tissue engineering of cartilage. Nat Mater. 2007; 6:162–7. [PubMed: 17237789]
25. Uquillas JA, Akkus O. Modeling the electromobility of type-I collagen molecules in the electrochemical fabrication of dense and aligned tissue constructs. Ann Biomed Eng. 2012; 40:1641–53. [PubMed: 22314838]
26. Cheng X, Gurkan UA, Dehen CJ, Tate MP, Hillhouse HW, Simpson GJ, et al. An electrochemical fabrication process for the assembly of anisotropically oriented collagen bundles. Biomaterials. 2008; 29:3278–88. [PubMed: 18472155]
27. Liu F, Kozanek M, Hosseini A, Van de Velde SK, Gill TJ, Rubash HE, et al. In vivo tibiofemoral cartilage deformation during the stance phase of gait. J Biomech. 2010; 43:658–65. [PubMed: 19896131]

28. Appelman TP, Mizrahi J, Elisseeff JH, Seliktar D. The differential effect of scaffold composition and architecture on chondrocyte response to mechanical stimulation. Biomaterials. 2009; 30:518–25. [PubMed: 19000634]
29. Hutmacher DW, T.; Dalton, PD.; Lewis, JA. Scaffold design and fabrication in tissue engineering. In: van Blitterswijk, C.; Thomsen, P.; Hubbell, J.; Cancedda, R.; de Bruijn, J.; Lindahl, A.; Sohier, J.; Williams, DF., editors. Tissue Engineering. London: Elsevier Academic Press; 2008. p. 403-54.
30. Lien SM, Ko LY, Huang TJ. Effect of pore size on ECM secretion and cell growth in gelatin scaffold for articular cartilage tissue engineering. Acta biomaterialia. 2009; 5:670–9. [PubMed: 18951858]
31. Stoop R. Smart biomaterials for tissue engineering of cartilage. Injury. 2008; 39(Suppl 1):S77–87. [PubMed: 18313475]
32. Athanasiou KAD, EM.; Hu, JC. Articular cartilage tissue engineering. In: Athanasiou, KA.; L, JK., editors. Synthesis Lectures on Tissue Engineering: Morgan & Claypool. 2009. p. 1-182.
33. Athanasiou KA, Agarwal A, Dzida FJ. Comparative-Study of the Intrinsic Mechanical-Properties of the Human Acetabular and Femoral-Head Cartilage. Journal of Orthopaedic Research. 1994; 12:340–9. [PubMed: 8207587]
34. Liao IC, Moutos FT, Estes BT, Zhao X, Guilak F. Composite three-dimensional woven scaffolds with interpenetrating network hydrogels to create functional synthetic articular cartilage. Adv Funct Mater. 2013; 23:5833–9. [PubMed: 24578679]
35. Hall, BK. Bones and cartilage: developmental and evolutionary skeletal biology. San Diego: Elsevier Academic Press; 2005. The membranous skeleton: condensations.
36. Dessau W, von der Mark H, von der Mark K, Fischer S. Changes in the patterns of collagens and fibronectin during limb-bud chondrogenesis. Journal of embryology and experimental morphology. 1980; 57:51–60. [PubMed: 7000961]
37. Kirsch T, von der Mark K. Ca2+ binding properties of type X collagen. FEBS letters. 1991; 294:149–52. [PubMed: 1743285]
38. Kirsch T, von der Mark K. Isolation of human type X collagen and immunolocalization in fetal human cartilage. European journal of biochemistry/FEBS. 1991; 196:575–80. [PubMed: 2013280]
39. Kirsch T, Ishikawa Y, Mwale F, Wuthier RE. Roles of the nucleational core complex and collagens (types II and X) in calcification of growth plate cartilage matrix vesicles. The Journal of biological chemistry. 1994; 269:20103–9. [PubMed: 8051098]
40. Kirsch T, Wuthier RE. Stimulation of calcification of growth plate cartilage matrix vesicles by binding to type II and X collagens. The Journal of biological chemistry. 1994; 269:11462–9. [PubMed: 8157677]
41. Beninghoff A. Form und bau der gelenkknorpel in ihren beziehungen zur funktion. Z Anat Entwicklungsgesch. 1925; 76:43.
42. He B, Wu JP, Kirk TB, Carrino JA, Xiang C, Xu J. High-resolution measurements of the multilayer ultra-structure of articular cartilage and their translational potential. Arthritis research & therapy. 2014; 16:205. [PubMed: 24946278]
43. Clark JM. The organization of collagen in cryofractured rabbit articular cartilage: a scanning electron microscopic study. Journal of orthopaedic research: official publication of the Orthopaedic Research Society. 1985; 3:17–29. [PubMed: 3981292]
44. Changoor A, Nelea M, Methot S, Tran-Khanh N, Chevrier A, Restrepo A, et al. Structural characteristics of the collagen network in human normal, degraded and repair articular cartilages observed in polarized light and scanning electron microscopies. Osteoarthritis and cartilage/OARS, Osteoarthritis Research Society. 2011; 19:1458–68.

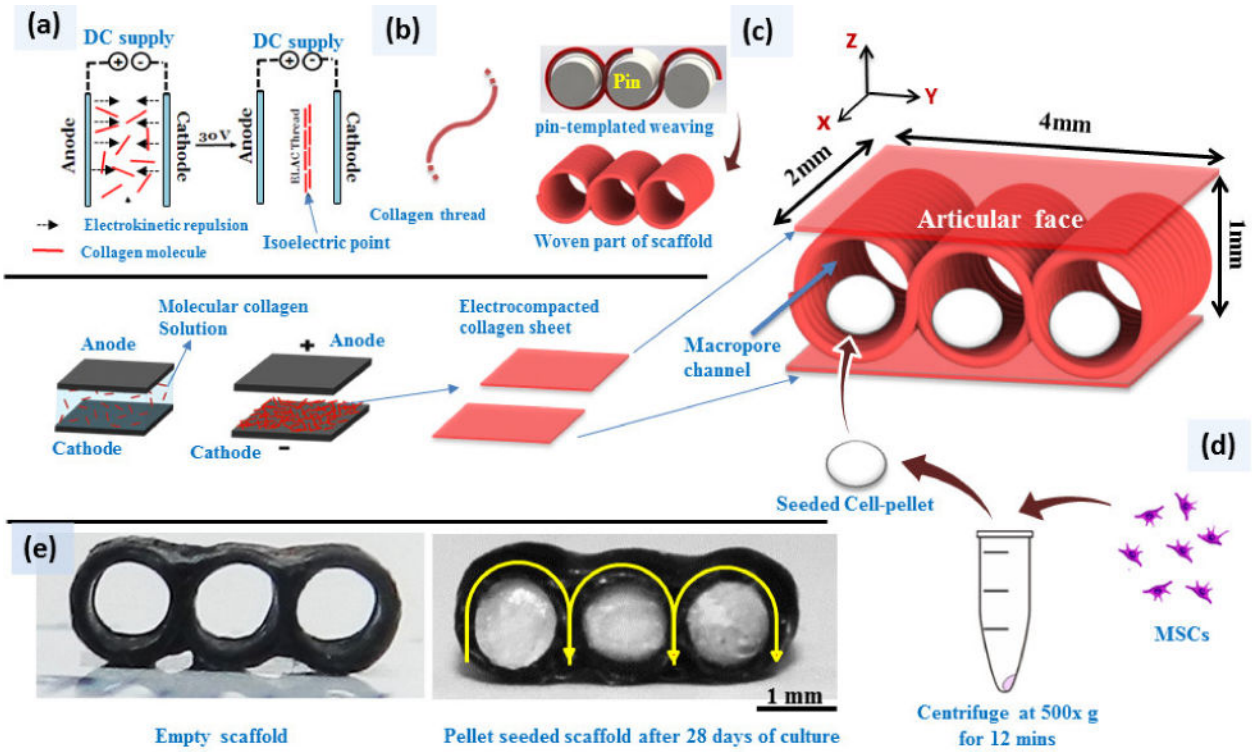

Figure 1.

Fabrication of macroporous woven scaffolds and pellet delivery via the macroporous woven collagen scaffold; (a) Liquid to solid phase transition of collagen molecules via electrocompaction to fabricate electrochemically aligned collagen threads and electrocompacted sheets. (b) Collagen thread is woven around a set of pins and threads are stabilized by crosslinking two collagen sheets on top and bottom of woven part of scaffold. (c) Schema of the final woven collagen scaffold. (d) 1 million MSCs pelletized at 500 ×g for 12 minutes, cultured for 3 days and then transferred in to scaffold holes.

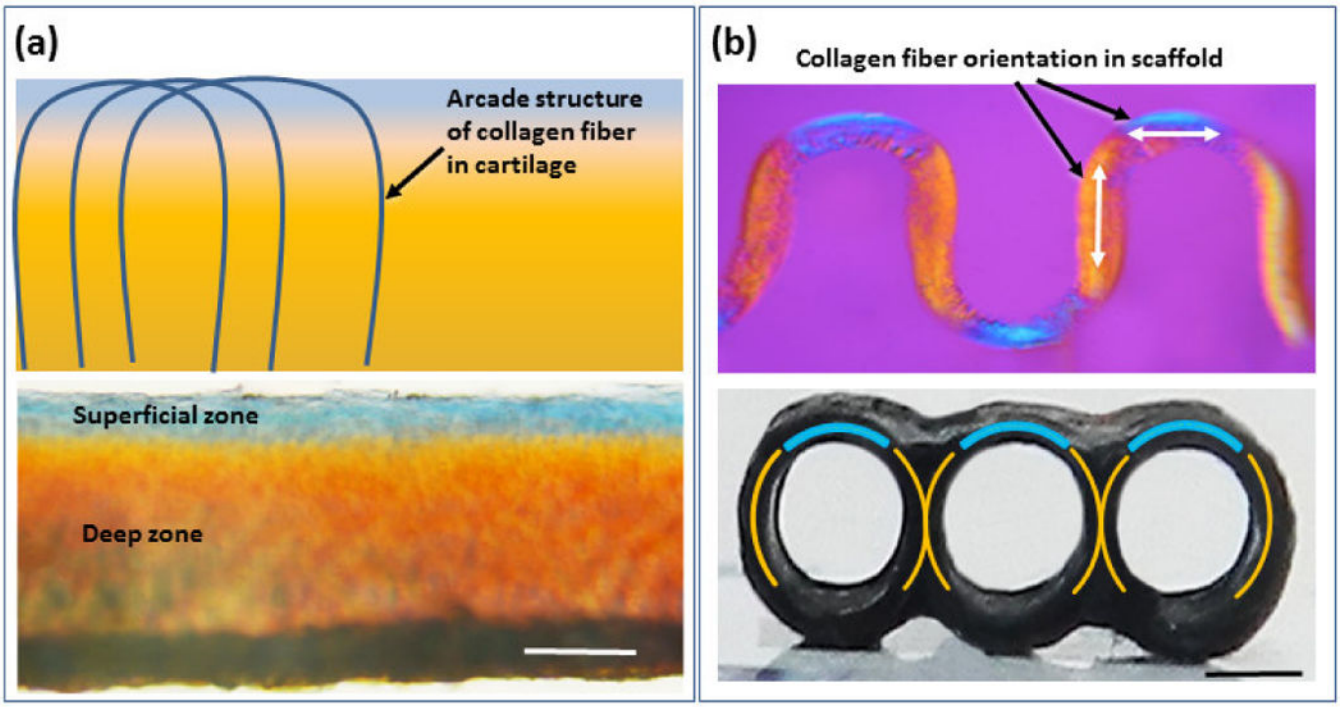

Figure 2.

Polarized optical microscopy illustrates the similarities in the orientations of the collagen fibers in native articular cartilage and woven collagen scaffold. Schematic depiction of arcade like structures formed by the changing orientation of collagen fibers in the articular cartilage [41–44]. Collagen fibers are oriented parallel to the surface of cartilage in the superficial region and in deeper zones the orientation changes to vertical orientation (a), this variation of the orientation of collagen fibers are manifested in blue in the superficial region and orange color in deep zone (a) as well as in woven scaffold which mimic the collagen fiber orientation of the native articular cartilage (b). (Scale bars: 500 μm).

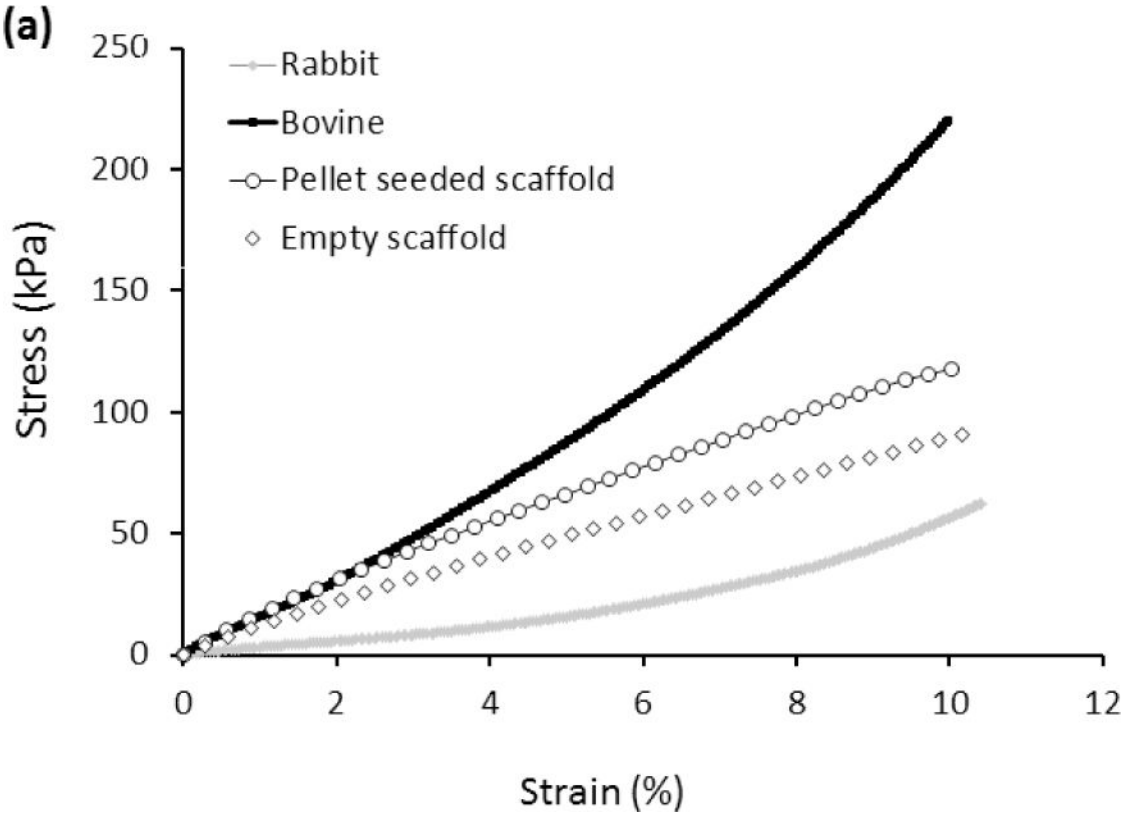

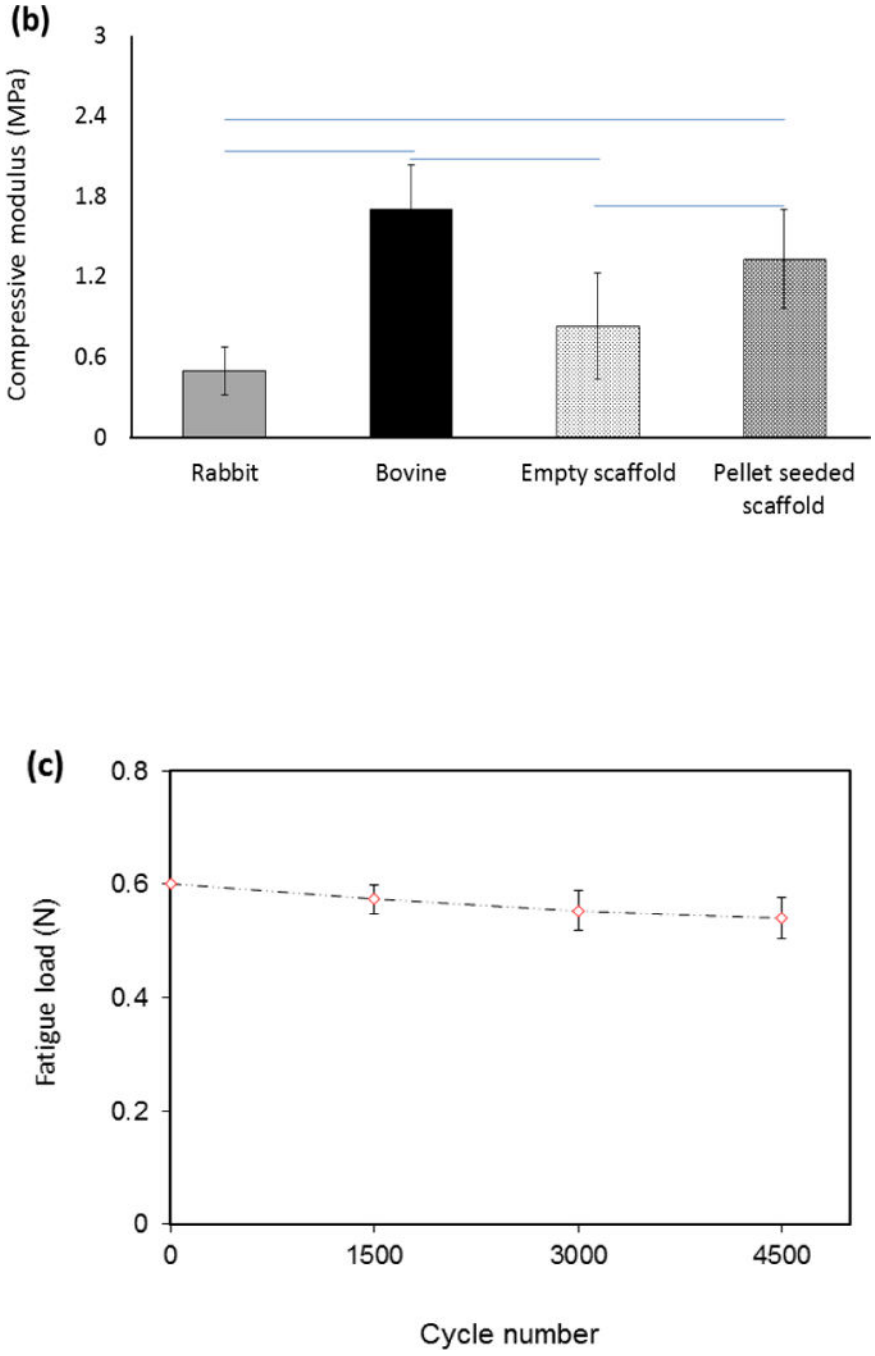

Figure 3.

(a) Mechanical characterization of the woven cartilage scaffold. Comparison of stress-strain curves of woven scaffold with rabbit and bovine cartilage. The strength of the scaffold is situated between rabbit and bovine cartilage. (b) Young's modulus of cells seeded scaffold was greater than that of the blank scaffold and did not differ significantly from that of bovine cartilage. The horizontal lines between individual groups represent statistically significant difference based on one way ANOVA test with Tukey's pairwise comparison

($p<0.05$). (c) Decrease in fatigue load of the scaffold under constant strain (15%) up to 4500 load cycles. Fatigue load decreases by about 8% after 4500 cycles.

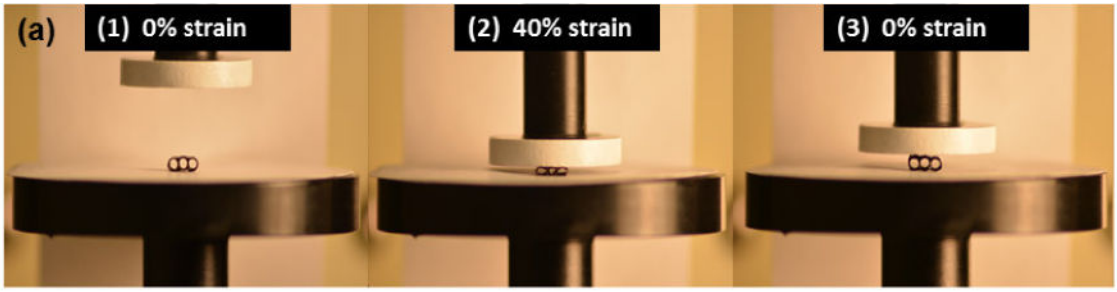

Figure 4a.

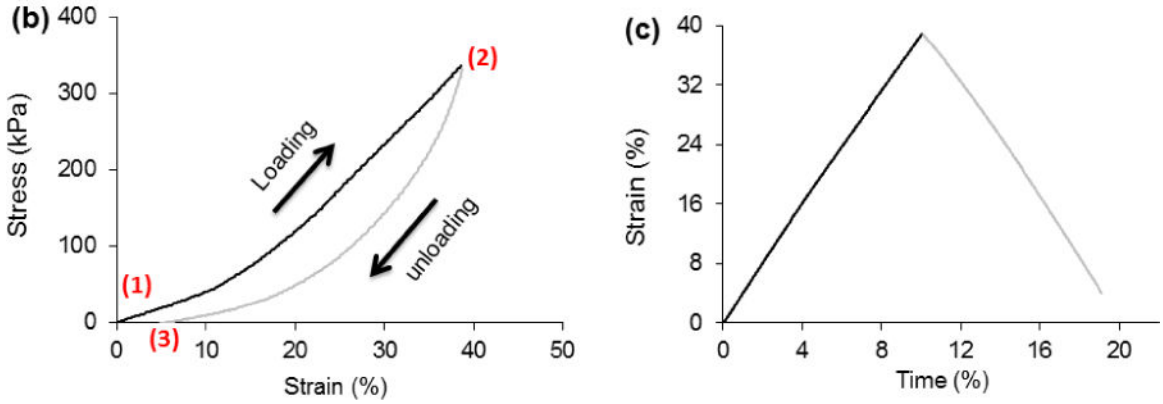

Figure 4.

Woven scaffold has a high degree of resilience. Loading and unloading the scaffold demonstrate that the scaffold shows only a small amount of permanent deformation following an overt strain of 40%. (a) Scaffold before loading (1), under 40% strain (2) and following unloading (3). (b) Typical stress-strain curve for a loading-unloading cycle. (c) The strain history indicates that the scaffold springs back to near its original height after being compressed about half its original thickness.

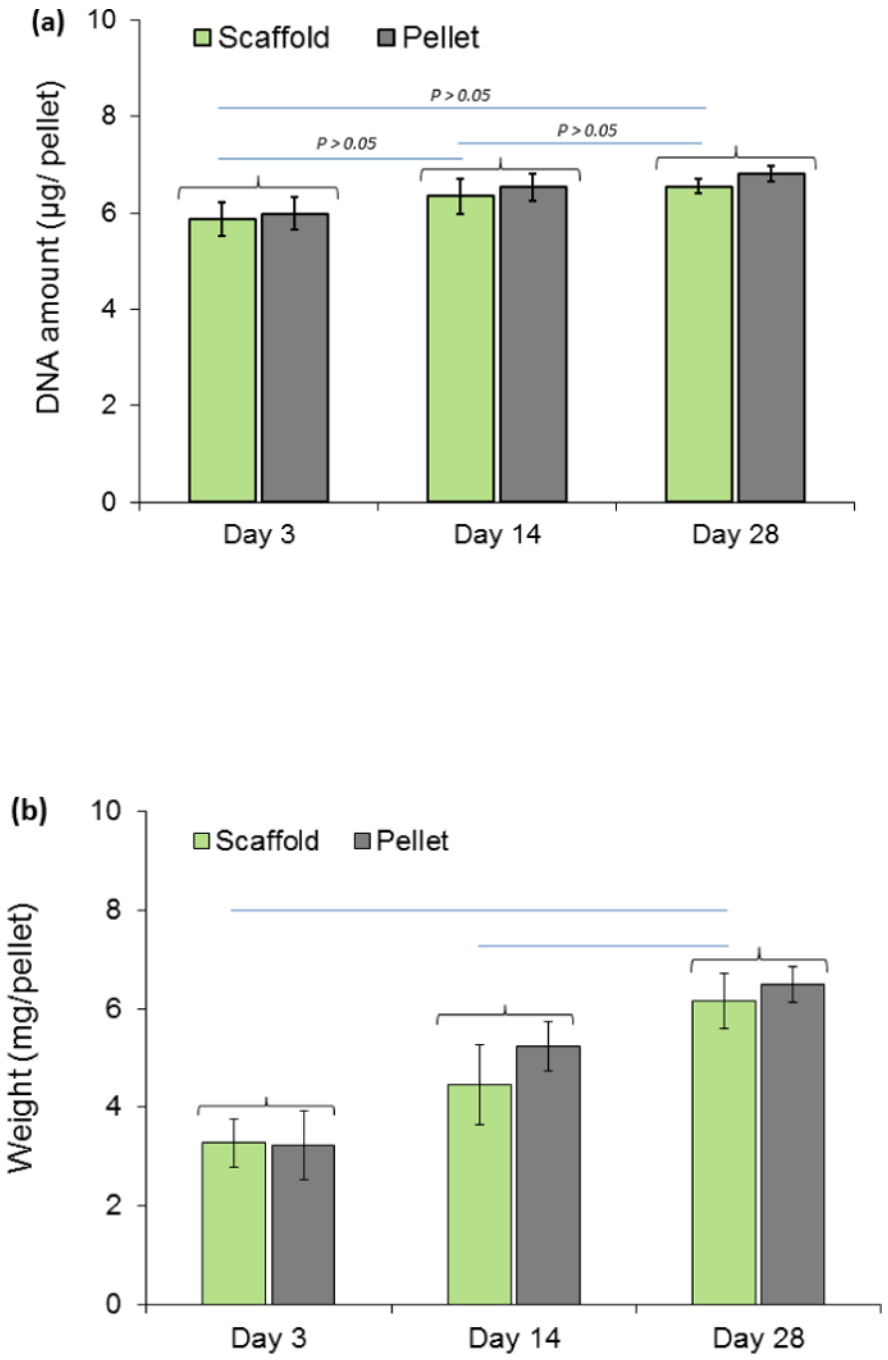

Figure 5.

(a) DNA content in free-standing vs. cell-seeded pellets, (b) increase in weights of pellet-seeded woven scaffold and free standing cell pellets during 4 weeks of culture period. Increases in weights of cell seeded scaffolds over time is statistically significant ($P<0.05$). Groups with significant difference are connected with horizontal line.

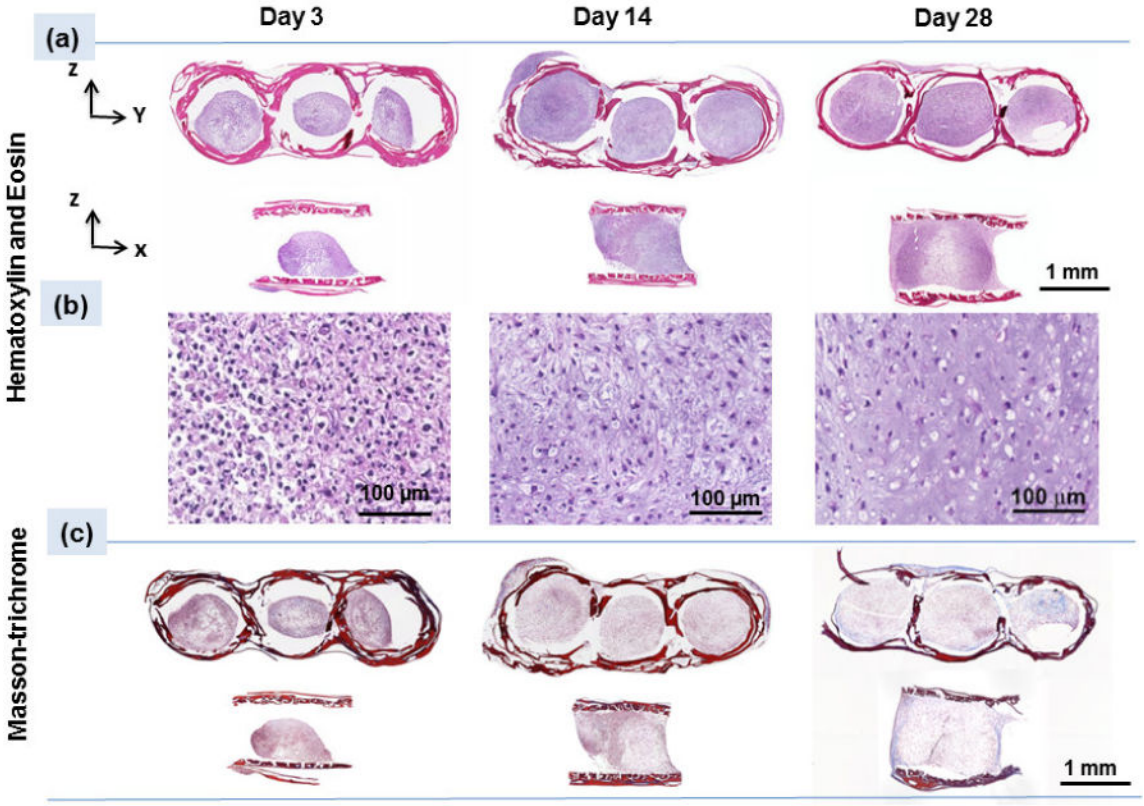

Figure 6.

(a) H&E staining of the scaffold on days 3, 14 and 28 indicate enlargement of pellets inside the scaffold, (b) High magnification images at different time points of day 3, 14, and 28 demonstrate cells round morphologies which over time spaces between the cells increase and filled with extra cellular matrix, (c) Masson-trichrome staining (blue color) illustrates increasing collagen content over 28 days of culture with increasing the blue color intensity.

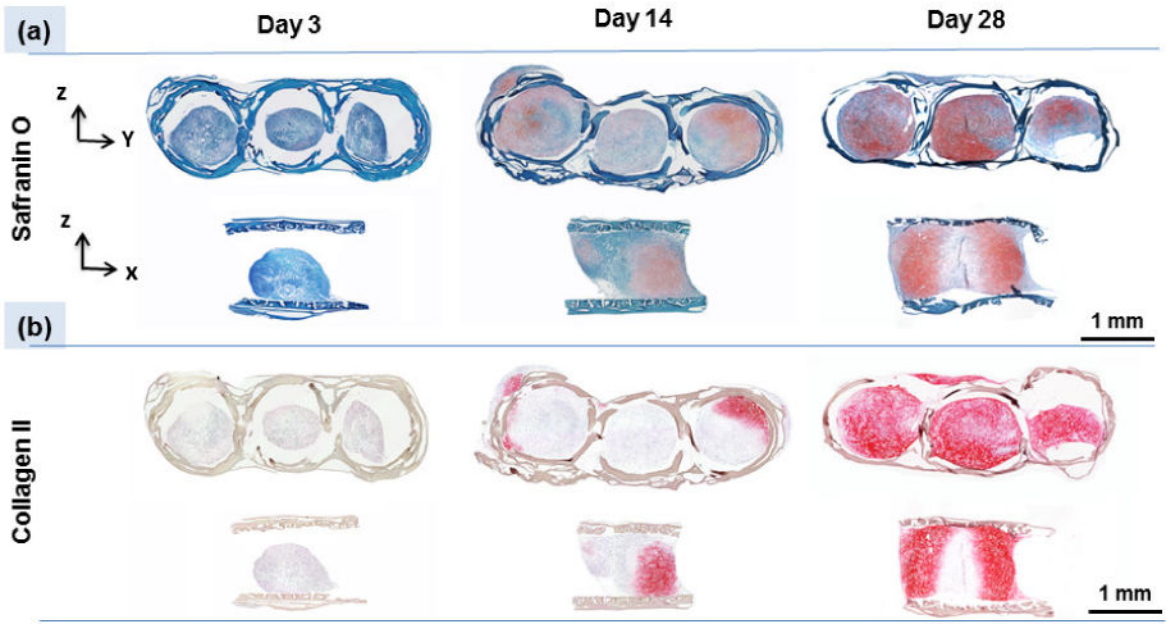

Figure 7.

Histology and immunohistochemistry of the scaffold on days 3, 14 and 28 indicate chondrogenesis taking place inside scaffolds. (a) Safranin O staining shows increasing GAGs production by cells over time, and (c) immuno-staining confirms the presence of type II collagen.

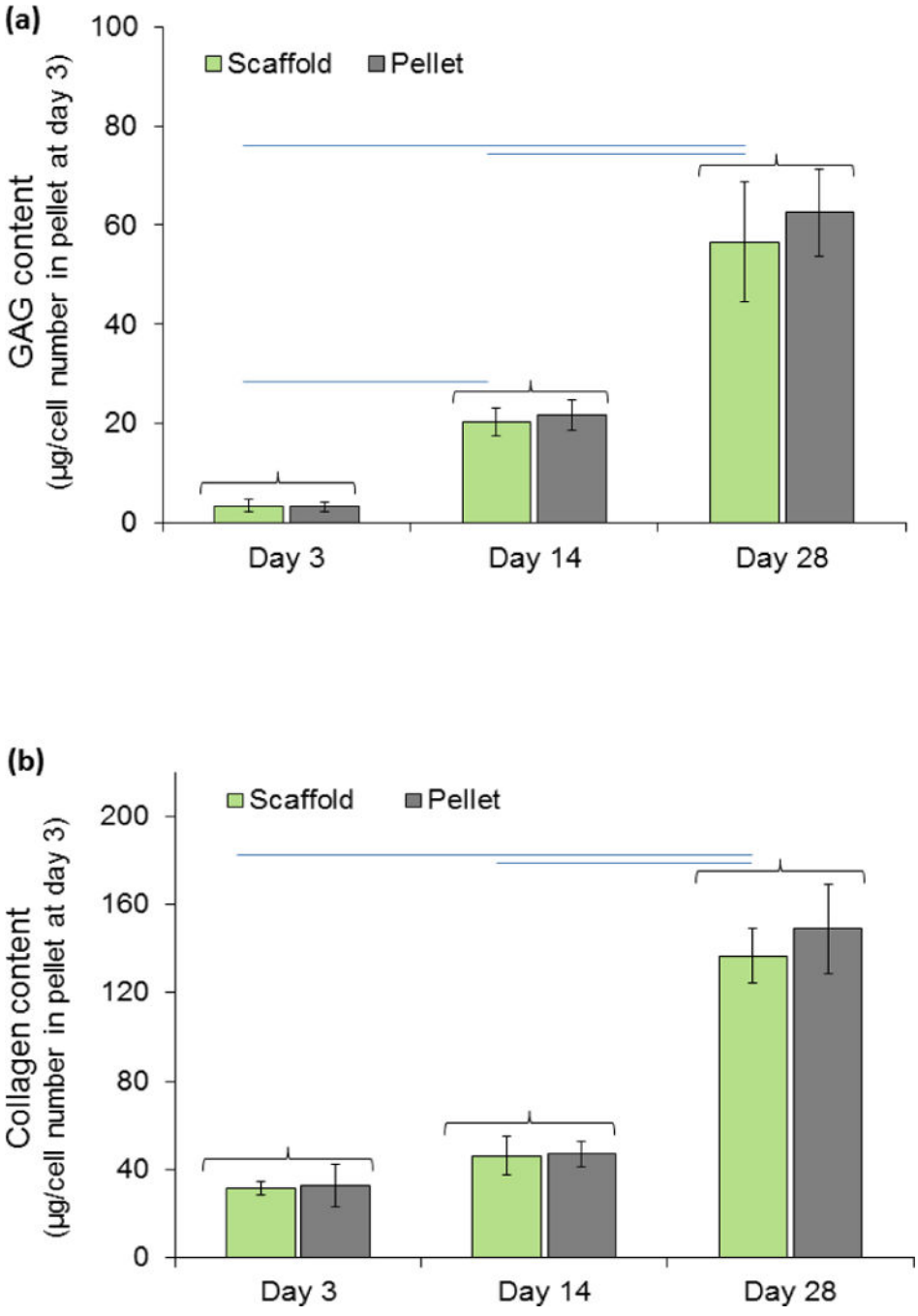

Figure 8.

Chondrogenesis of pellets seeded in scaffolds do not differ from free standing pellets. (a) Glycosaminoclycans (GAGs) and (b) collagen production by pellets within woven scaffold and free standing pellets increased during the 4 weeks of *in-vitro* culture. *In-vitro* results show woven scaffold supports chondrogenesis and extracellular matrix production by the pellets within scaffolds is similar to that by free-standing positive control pellets. Amount for GAGs and collagen presented in graphs are normalized to the amount of DNA. There were not any significant differences between pellet and cell seeded scaffold at each time

point for all properties. Increases in GAGs and collagen production of cell seeded scaffold over time is statistically significant ($P<0.05$). Groups with significant difference are connected with horizontal line. Error bars show standard deviation.

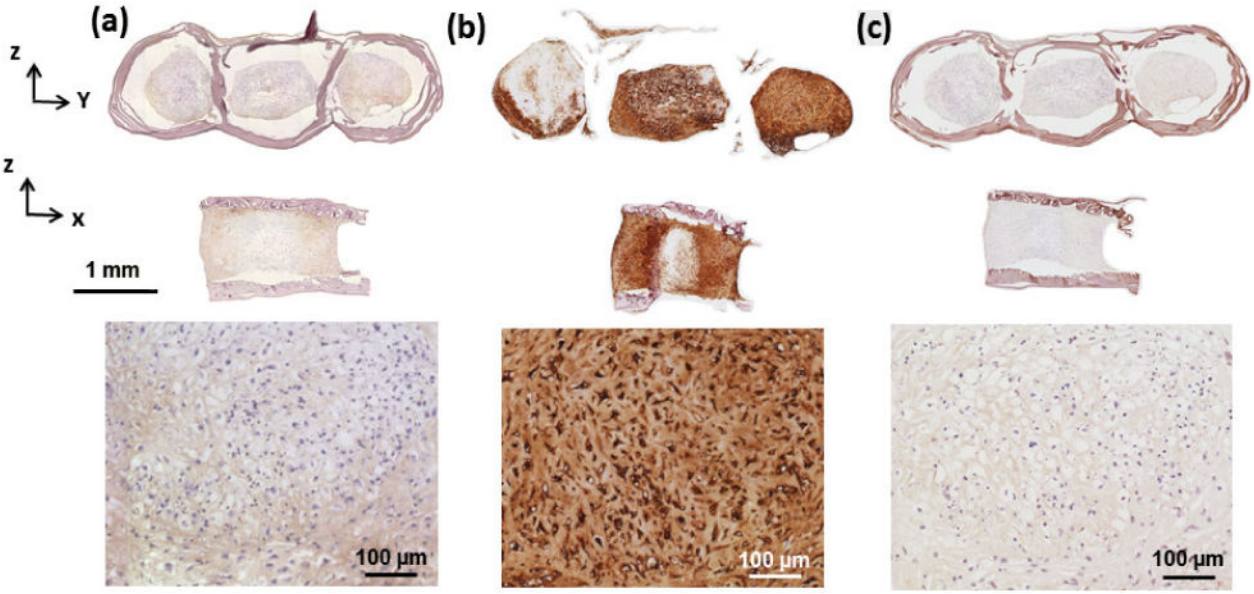

Figure 9.

Immunostaining at day 28 of culture showed MSCs differentiating to chondrogenic lineage. (a) Immunostaining of the scaffold for collagen type I is slightly positive. (b) Strong presence of aggrecan was evident as a cartilage specific molecule in cell pellets. (c) Negative immunostaining for collagen X in cell pellet.

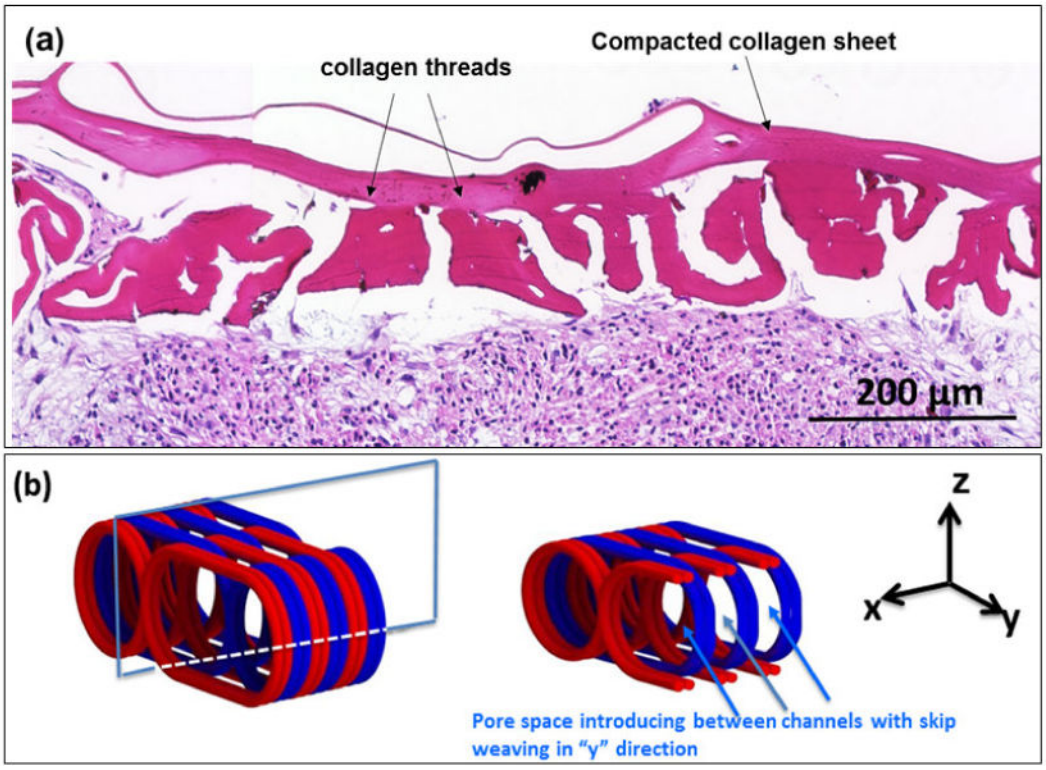

Figure 10.

(a) H&E staining demonstrates the integration of pellet boundaries with the scaffold walls. To improve the existing weaving pattern, in next generation of the scaffold (b) channels will be connected with lateral pores based on the designed skip-weaving pattern. The left image in 'b' demonstrate scaffolds with three channels. The cross sectional plane in the XZ shows the interface between two neighboring channels. The view of this interface from y axis shown in the right.